VI. RADIO ASTRONOMY*

Academic and Research Staff

Prof. A. H. Barrett
Prof. B. F. Burke
Prof. L. B. Lenoir
Prof. D. H. Staelin
Dr. S. H. Zisk
J. W. Barrett
Patricia P. Crowther
E. R. Jensen
P. L. Seymour

Graduate Students

R. J. Allen
M. S. Ewing
N. E. Gaut
M. Melnick
J. M. Moran, Jr.
G. D. Papadopulos
E. C. Reifenstein III
A. E. E. Rogers
K. D. Thompson
T. L. Wilson

RESEARCH OBJECTIVES AND SUMMARY OF RESEARCH

The research objectives of the Radio Astronomy Group may be broadly described as follows.

1. Studies of continuum emission of extraterrestrial radio sources. The antenna facilities of the Haystack Microwave Research Facility, Lincoln Laboratory, M.I.T., have been used at 2-cm and 3.75-cm wavelengths to study temporal variations in the radio flux from quasi-stellar radio sources,[1] to map the brightness distribution in both the polarized and unpolarized components of the radiation from the strong radio sources,[2] and to determine the absolute flux from the radio sources Cassiopeia A and Taurus A.[3] This work continues and is being extended to other sources. The National Radio Astronomy Observatory interferometer, Green Bank, West Virginia, has been used for determining the brightness distribution of many galatic and extragalatic radio sources at 234 Mc/sec. Studies of Venus and Jupiter at wavelengths near the water-vapor and ammonia resonances have been carried out on the 28-ft radio telescope of Lincoln Laboratory.[4] A radiometer operating at 4-mm wavelength has been installed and tested on the 29-ft radio telescope at the Prospect Park Field Station of Air Force Cambridge Research Laboratories, and planetary observations are planned for the near future.

2. Studies of the radio spectrum of the interstellar medium. The spectral lines of OH have been the subject of extensive observations with the antennas of the Haystack Microwave Research and Millstone Radar Facility, Lincoln Laboratory, M.I.T., and the 140-ft radio telescope of the National Radio Astronomy Observatory, Green Bank, West Virginia. The studies during the past year have led to (a) the detection of circularly polarized OH emission,[5] (b) the detection of the isotopic species $O^{18}H$,[6] and the establishment of an upper limit to the angular size of the OH emitting regions of 15 seconds of arc.[7] Interferometric observations are being extended by using the Millstone and Agassiz (Harvard) radio telescopes as an interferometer to determine the angular size of the emission regions. Searches for other spectral lines are concentrating on the CH radical, with a line expected near 3300 Mc/sec.

3. Study of microwave emission and absorption by the terrestrial atmosphere and

*This work was supported principally by the National Aeronautics and Space Administration (Grant NsG-419 and Contract NSR-22-009-120); and in part by the Joint Services Electronics Programs (U.S. Army, U.S. Navy, and U.S. Air Force under Contract DA 36-039-AMC-03200(E).

surface, with particular emphasis on the meteorological satellite application of microwave sensors. This work has included ground-based observations in conjunction with, and in support of, measurements of planetary microwave emission, and theoretical studies of satellite measurements of atmospheric water vapor and oxygen. An extensive program of balloon observations has been carried out to determine the microwave properties of the upper atmosphere as governed by the resonance lines of molecular oxygen at 5-mm wavelength.[8] These results indicate departures from the Van Vleck-Weisskopf theory of microwave absorption and emission, and further observations are being made to confirm this conclusion. Observations of the water-vapor resonance at 1.35 cm in the terrestrial atmosphere have also been carried out.[9]

A. H. Barrett

References

1. R. J. Allen and A. H. Barrett (to appear in Astron J., November 1966 issue).
2. R. J. Allen and A. H. Barrett, paper presented ath the 123rd Meeting of the American Astronomical Society, Los Angeles, California, December 27-30, 1966.
3. R. J. Allen and A. H. Barrett (to appear in Astron. J., November 1966 issue).
4. D. H. Staelin and R. W. Neal (to appear in Astron. J., November 1966 issue).
5. A. H. Barrett and A. E. E. Rogers, Nature 210, 188 (1966).
6. A. E. E. Rogers and A. H. Barett (to appear in Astron. J., November 1966 issue).
7. A. E. E. Rogers, J. M. Moran, P. P. Crowther, B. F. Burke, M. L. Meeks, J. A. Ball, and G. M. Hyde, Phys. Rev. Letters 17, 450 (1966).
8. A. H. Barrett, J. W. Kuiper, and W. B. Lenoir, J. Geophys. Res. 71, 4723 (1966).
9. D. H. Staelin, J. Geophys. Res. 71, 2875 (1966).

A. HAYSTACK-MILLSTONE OH INTERFEROMETER

Observations of OH emission with an interferometer comprising the Haystack (120-ft) and Millstone (84-ft) antennas have been reported previously.[1] The results can now be extended to include the positions and angular sizes of the emission regions associated with W49, NGC 6334 and Sagittarius, as shown in Table VI-1. The region in Sagittarius was observed to be a point source. W49 is seen to be a double source, whose components remain unresolved. NGC 6334 is at least a double source, but may be more complex. Only one of the components of NCG 6334 was mapped with the interferometer, owing to the poor signal-to-noise ratio and the limited hour angle availability for their source.

Table VI-1. Position and angular sizes of OH emission regions.

Line[a] Velocity km/sec	Polarization	Fringe Amplitude Observed	Effective Source Diameter	Separation from Line with Position Listed	Position-Epoch 1950 α	Position-Epoch 1950 δ
W3 1665 MHz	June 7, 8, 9, 10, 11, 12, 13	July 9, 11	±12 hr			
-45.1	right	1.0 ±0.05	<15"		$02^h23^m16.3\pm1^s$	61°38'57±5"
-43.7	right	1.0 ± 0.1	<20"	<3"		
-41.7	right	1.0 ± 0.2	<25"	<3"		
-45.4	left	1.0 ± 0.1	<20"	<3"		
-46.4	left	1.0 ± 0.1	<20"	<3"		
W3 1667 MHz	June 12, 29	July 8, 9	±12 hr			
-42.3	right	1.0 ± 0.3	<30"	<7"		
-44.8	left	1.0 ± 0.3	<30"		<15" from 1665 Position	
W49 1665 MHz	Position 1	June 29	July 10	±6 hr		
17.0	right	0.9 ± 0.2[b]		<7"		
5.5	left	1.0 ± 0.2	<25"	<15"		
12.0	left	1.0 ± 0.2	<25"	<10"		
16.8	left	0.8 ± 0.3[b]		<7"		
20.9	left	1.0 ± 0.1	<20"		$19^h7^m49.7\pm1^s$	9°1'12±5"
W49 1667 MHz	Position 1	July 8, 9	±6 hr			
2.0	right	1.0 ± 0.3	<30"	<7"		
5.0	right	1.0 ± 0.2	<25"		<7" from 1665 Position 1	
3.0	left	1.0 ± 0.2	<25"	<7"		
5.0	left	1.0 ± 0.21	<20"	<7"		
19.0	left	0.6 ± 0.4[b]		<7"		
W49 1665 MHz	Position 2					
16.0	right	0.8 ± 0.2[b]		<7"		
15.7	left	1.0 ± 0.2	<25"			+8.5[s] R.A.
17.9	left	0.± ± 0.3[b]		<7"		-68" Dec. from Pos. 1
W49 1667 MHz	Position 2					
19.0	left	0.6 ± 4[b]			<10" from 1665 Position 2	
NGC 6334 1665 MHz	July 11, 12	±2 hr				
-12.4	right	1.0 ± 0.2	<25"		$17^h17^m33.5\pm2^s$	-35°45'35±10"
-9.1	left	1.0 ± 0.2	<25"	<7"		
SAG (W24) 1665 MHz	July 10, 11	±3 hr				
74.0	right	1.0 ± 0.2	<25"	<7"	[1] $17^h44^m11\pm2^s$	-28°23'29±10"
67.5	left	1.0 ± 0.1	<20"			

[a]Line velocity based on Radford's (1964) rest frequencies for the $2\pi_{3/2}$, J = 3/2, Λ - doublet of $O^{16}H^1$.

[b]Features that show a systematic fringe amplitude variation.

Most measurements were made with a frequency resolution of 3 kHz; some of the W3 measurements were made with 1 kHz.

None of the components of any OH source is yet resolved, and measurements are now being extended to a longer baseline, in cooperation with the Harvard Agassiz Station (see Sec. VI-B).

B. F. Burke, J. M. Moran, A. E. E. Rogers

References

1. B. F. Burke, J. M. Moran, and A. E. E. Rogers, Quarterly Progress Report No. 83, Research Laboratory of Electronics, M.I.T., October 15, 1966, pp. 7-9.

B. MILLSTONE-AGASSIZ OH INTERFEROMETER

Previous OH interferometer observations, as described in Section VI-A, have clearly demonstrated the need for observations with a larger baseline than the 3800 λ available with the Haystack-Millstone complex. This has led to a joint experiment, involving Research Laboratory of Electronics, Lincoln Laboratory, and Harvard personnel, in which the 84-ft antenna of the Millstone Radar Facility and the 60-ft radio telescope of the George R. Agassiz Radio Astronomy Station of Harvard College Observatory is being used as an interferometer. The telescopes are separated by 74,390 λ (43,925 ft) along a line oriented 22.52° East of North. Phase coherence is maintained by use of a one-way microwave link operating at 7325 Mc/sec on a line-of-sight path between the two stations. The Harvard radiometer has a maser preamplifier and a system temperature of 140°K; the Millstone radiometer has a tunnel-diode amplifier and a system temperature of approximately 700°K. The essential features of the data reduction are the same those as used in the Millstone-Haystack experiment. The OH source W3 has been examined with a bandwidth of 120 kc/sec and a resolution of 3 kc/sec. Preliminary observations have revealed fringes at 1665 Mc/sec.

A. H. Barrett, B. F. Burke, J. M. Moran, A. E. E. Rogers

C. K-BAND SPECTRUM MEASUREMENTS OF THE SUN

The solar brightness spectrum near 1-cm wavelength was measured on several days in the period January-March, 1966. The measurements were made with the Lincoln Laboratory 28-ft millimeter antenna and the Research Laboratory of Electronics 5-channel K-band radiometer.[1] The frequencies observed were 19.0, 21.0, 22.2, 23.5, and 25.5 GHz. This solar band had not been carefully studied before.

The measurements were made by taking drift scans across the center of the sun every 10 minutes for a period of approximately 2 hours each day. The resulting measurements were corrected for atmospheric absorption by extrapolation to zero atmosphere

the observed dependence of solar intensity upon elevation angle.

The results were calibrated by comparison of the solar data with the average lunar brightness temperature observed over a lunation. The comparison was made using the antenna patterns measured at each frequency.[1] The true lunar brightness temperature was estimated from observations by many observers at many wavelengths.[2] The errors involved in this comparison technique are very nearly the same at each frequency and thus the relative errors are small. The relative errors were dominated by the effective receiver noise and system gain fluctuations present during the lunar and solar observations. If it is assumed that the true average lunar brightness temperature is known within 5 per cent, the absolute rms error at each frequency is approximately ±700°K.

The measured average solar brightness temperatures of the center of the sun are listed in Table VI-2, together with the relative rms errors. Only the eight most accurate

Table VI-2. Observed K-band solar spectrum.

Frequency (GHz)	Central Solar Brightness Temperature (°K)	Relative rms Error (°K)
19.0	10,800	±400
21.0	10,800	±400
22.2	11,000	±500
23.5	10,700	±500
25.5	9,800	±300

spectra were averaged. The rest of the data is not included here.

This average spectrum is composed of data obtained on February 10, 18, 23, and 24, and March 3, 10, 11, and 14, 1966. The spectrum did not appear to vary much over this period. These results superseded the data presented earlier,[3] which were based on incomplete calibration data.

D. H. Staelin, N. Gaut, Sara Law, W. T. Sullivan III.

References

1. D. H. Staelin, "Microwave Spectrum of Venus," Sc. D. Thesis, Department of Electrical Engineering, M.I.T., 1965.

2. J. M. Moran, "Radiometric Observations of the Moon near One-Centimeter Wavelength," S.M. Thesis, Department of Electrical Engineering, M.I.T., 1965.

3. W. T. Sullivan III, "Solar Observations at Millimeter Wavelength," NEREM Record (1966), IEEE Cataloge No. F-70.

D. INFERENCE OF ATMOSPHERIC ATTENUATION NEAR 61.15 GHz FROM BALLOON FLIGHT RESULTS

Balloon Flight Experiments such as the 154-P series, which have been previously reported,[1] (see also Sec. VI-F), yield data that can be used to infer the atmospheric attenuation coefficient as a function of height. The ascent and descent portions of the flight are useful in this respect when coupled with accurate measurements of the atmospheric temperature and pressure.

The appropriate measurement geometry is shown in Fig. VI-1. The assumptions made in this inversion method are that the atmosphere may be modeled by infinite planar

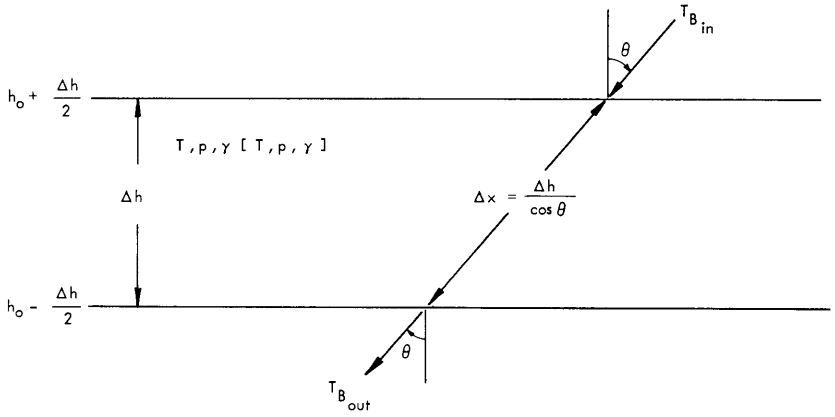

Fig. VI-1. Geometry of the measurements.

layers (valid for $\theta \lesssim 80°$), and within a layer the temperature and pressure may be taken as constant (valid for $\Delta h \lesssim 2.5$ km). The equation of transfer relating the brightness temperatures, $T_{B\,in}$ and $T_{B\,out}$, is

$$T_{B\,out} = T_{B\,in} \exp\left(-\gamma(h_o)\frac{\Delta h}{\cos\theta}\right) + T\left[1-\exp\left(-\gamma(h_o)\frac{\Delta h}{\cos\theta}\right)\right]. \tag{1}$$

This relation can be solved for $\gamma(h_o)$:

$$\gamma(h_o) = \frac{\cos\theta}{\Delta h} \ln\left|\frac{T - T_{B\,in}}{T - T_{B\,out}}\right|, \tag{2}$$

under the assumption that the quantities on the right of (2) are known.

In balloon experiments such as 154-P, the antenna temperature (see Sec. VI-C) is measured, not the brightness temperature. In order to infer the value of $\gamma(h_o)$, the

antenna temperatures at $h_o \pm \frac{\Delta h}{2}$ must be converted to the brightness temperatures along the antenna axis at $h_o \pm \frac{\Delta h}{2}$. The results of flight 154-P indicate a true (measured) antenna temperature that is different from (higher than) the computed values for heights at which the optical depth is not large (that is, at heights above where $T_A = T_B = T$). This would appear to indicate that the true absorption coefficient is higher than the one used in the computations.

Fig. VI-2 shows the mechanics of converting the measured antenna temperatures into brightness temperatures. This conversion is built around the assumption that the

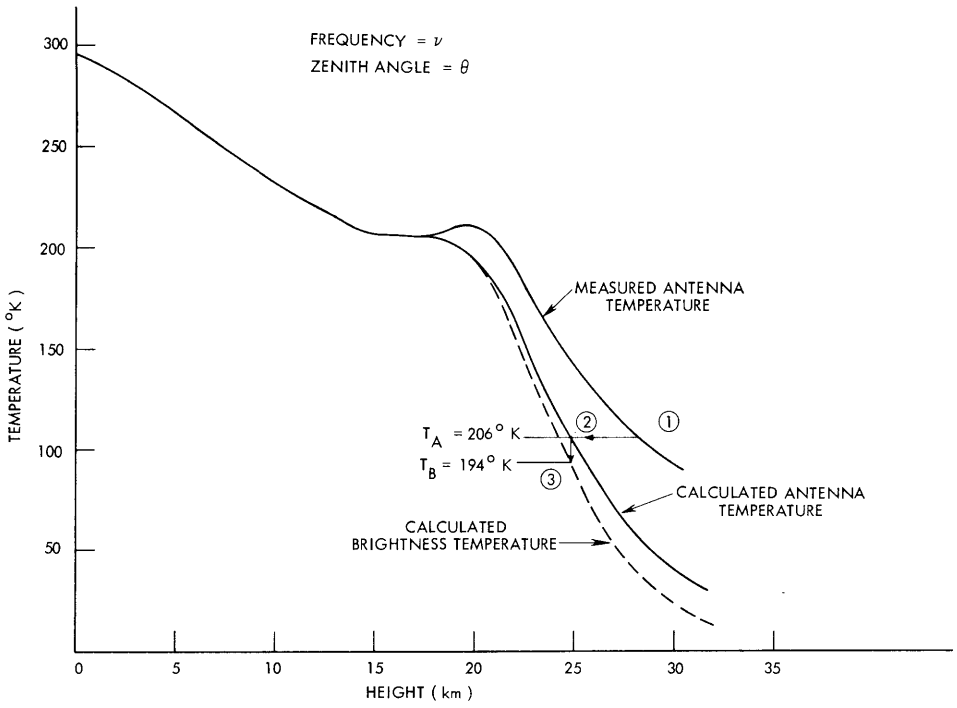

Fig. VI-2. Mechanics of antenna temperature to brightness conversion.

brightness distribution determining a given antenna temperature is the same for the measured antenna temperature and for the computed one. That is, changing the absorption coefficient merely moves the brightness distributions around in height but does not change them. The validity of this assumption can be checked. Thus (in Fig. VI-2) an antenna temperature of 206°K, measured at 28 km is converted to a brightness temperature of 194°K, which is assumed to be appropriate at 28 km.

The effects of noise and uncertainty can be seen by making the following replacement in Eq. 2:

$$T \rightarrow T + \Delta T$$

$$T \rightarrow T_{B\,in} + \Delta T_{B\,in}$$

$$T \rightarrow T_{B\,out} + \Delta T_{B\,out}$$

which yield

$$\gamma(h_o) + \Delta\gamma = \frac{\cos\theta}{\Delta h}\left[\ln\left|\frac{T - T_{B\,in}}{T - T_{B\,out}}\right| + \ln\left|\frac{1 + \dfrac{\Delta T - \Delta T_{B\,in}}{T - T_{B\,in}}}{1 + \dfrac{\Delta T - \Delta T_{B\,out}}{T - T_{B\,out}}}\right|\right] \tag{3}$$

that can be expanded to yield

$$\Delta\gamma_{rms} = \frac{\cos\theta}{\Delta h}\left\{\left|\frac{T_{B\,in} - T_{B\,out}}{(T-T_{B\,in})(T-T_{B\,out})}\right| \Delta T_{rms} + \left[\frac{1}{|T - T_{B\,out}|} + \frac{1}{|T-T_{B\,in}|}\right] \Delta T_{B_{rms}}\right. \tag{4}$$

under

$$\left|\frac{\Delta T - \Delta T_{B\,in}}{T - T_{B\,in}}\right| \ll 1,$$

$$\left|\frac{\Delta T - \Delta T_{B\,out}}{T - T_{B\,out}}\right| \ll 1,$$

and ΔT, $\Delta T_{B\,in}$, and $\Delta T_{B\,out}$ are mutually independent and have rms values of ΔT_{rms}, $\Delta T_{B_{rms}}$, and $\Delta T_{B_{rms}}$, respectively.

The inferred absorption coefficient based on the results of 154-P are shown in Figs. VI-3 and VI-4. Layer thicknesses of 1 km and 2 km were used. The right-hand

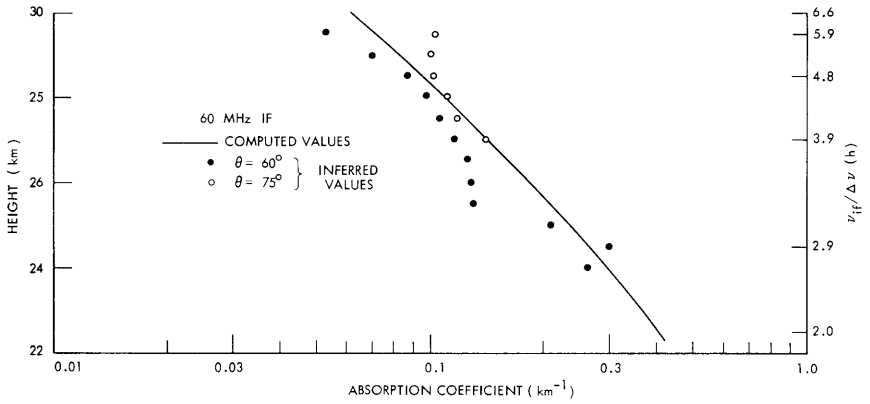

Fig. VI-3. Inferred absorption coefficients, Flight 154-P.

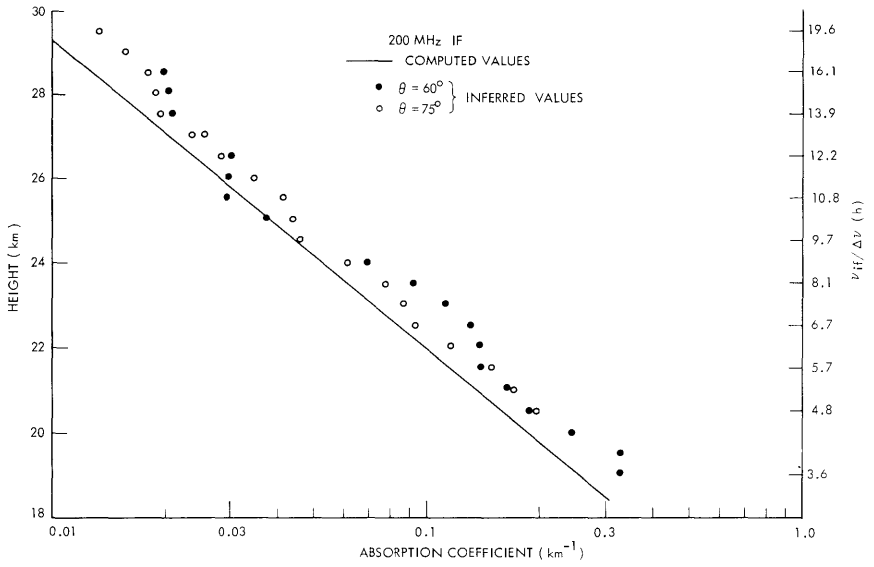

Fig. VI-4. Inferred absorption coefficients, Flight 154-P.

labeling of the vertical axis (essentially frequency in linewidth units) is given to facilitate comparison of inferred values with values computed on the basis of the Van Vleck-Weisskopf line-shape function

$$F(\nu) = \frac{1/\Delta\nu(h)}{\left(\frac{\nu - \nu_{9^+}}{\Delta\nu(h)}\right)^2 + 1}, \tag{5}$$

where $\nu - \nu_{9^+} = \pm\nu_{if}$, and $\Delta\nu$ is the linewidth.

If rms noise fluctuations of $\Delta T_{rms} = 1°K$ and $\Delta T_{B_{rms}} = 2°K$ are assumed, error bars on the inferred points will be approximately ±10-20%.

From Fig. VI-4 it is fairly evident that the absorption coefficient at frequencies well away from the resonance frequency is higher than theory predicts. Two possible changes in the theoretical line shape are being investigated as possible explanations of the higher absorption in the line wings.

The first is a change within the Van Vleck-Weisskopf line-shape theory. On the line-wings Eq. 5 can be expressed as

$$F(\nu) = \frac{\Delta\nu(h)}{(\nu - \nu_{9^+})^2}, \tag{6}$$

which indicates that the wing absorption can be increased by using a larger linewidth;

however, this results in a lower absorption near line center. Whether an absorption coefficient with this correction will adequately agree with the measured values over the entire height range is being investigated.

The second change under investigation is to go to a new line-shape theory. In particular, the impact theory of Gordon[2] should be looked at closely. In this theory it is not assumed that the absorption coefficient of overlapping resonance lines is the sum of the individual absorption coefficients.

Once a better expression for the absorption coefficient is obtained, theoretical computations of the brightness temperature distribution can be made to check the earlier assumption. Any necessary corrections can be made and the method repeated with the correct brightness temperatures.

W. B. Lenoir

References

1. W. B. Lenoir, Quarterly Progress Report No. 82, Research Laboratory of Electronics, M.I.T., July 15, 1966, pp. 36-41.
2. R. G. Gordon, J. Chem. Phys. 45, 1635-1655 (September 1, 1966).

E. OBSERVATIONS OF MICROWAVE EMISSION FROM ATMOSPHERIC OXYGEN: BALLOON FLIGHTS, SUMMER 1966

Two more balloon flight experiments were performed during August, 1966. The characteristics of these flights have been summarized in a previous report.[1] Preliminary analysis indicates that both flights were successful. Further analysis awaits the complete report from the balloon base.

W. B. Lenoir, J. W. Barrett, D. C. Papa

References

1. W. B. Lenoir, Quarterly Progress Report No. 82, Research Laboratory of Electronics, M.I.T., July 15, 1966, pp. 36-41.

F. OBSERVATIONS OF MICROWAVE EMISSION FROM ATMOSPHERIC OXYGEN: BALLOON EXPERIMENT RESULTS, SUMMER 1965

During July 1965, four balloon flight experiments were performed from the NCAR Balloon Base, Palestine, Texas. These flights (150-P, 152-P, 153-P, 154-P) have been described in previous reports.[1,2] Two distinct types of experiments were flown. Flights 150-P and 154-P were experiments to study the shape of the 9^+ resonance line,

Table VI-3. Summary of Flights 150-P and 154-P.

ν_o = 61.151 GHz (9^+ resonance line)

ν_{if} = center frequency of IF passband

B_{if} = bandwidth of IF passband

θ = zenith angle of antenna axis

ΔT_{rms} = output noise fluctuations (measured)

θ (deg)	ν_{if} (MHz)	B_{if} (MHz)	ΔT_{rms} (°K)
60	20	10	1.7
60	60	10	2.0
60	200	15	2.8
75	20	10	2.5
75	60	10	4.5
75	200	15	3.2

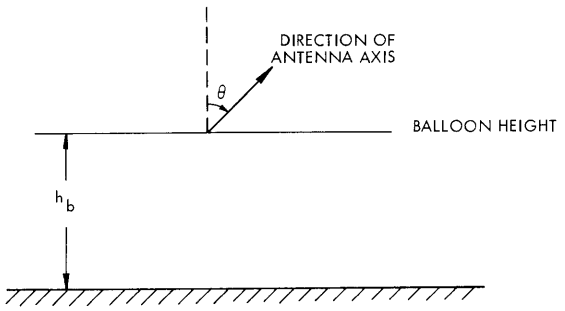

Fig. VI-5. Geometry of Flights 150-P and 154-P.

while flights 152-P and 153-P were experiments to remotely infer the atmospheric temperature profile below the balloon. Data analysis yielding the antenna temperatures of these flights has been completed.

1. Results of Flights 150-P and 154-P

Both of these flights had the same physical characteristics and geometry, as shown in Fig. VI-5 and Table VI-3. The measured quantity is the antenna temperature, T_A, which is the brightness temperature distribution weighted by the antenna gain pattern

$$T_A = \frac{1}{4\pi} \int_{4\pi} T_B(\theta, \phi)\, G(\theta, \phi)\, d\Omega(\theta, \phi), \tag{1}$$

with $G(\theta, \phi)$ being the known antenna gain, and $\Omega(\theta, \phi)$ the solid angle. The brightness

temperature at a zenith angle θ and a frequency ν is given by

$$T_B(\nu, \theta) = \int_{h_0}^{\infty} T(h)\, WF(h, \nu, \theta)\, dh, \tag{2}$$

with

$$WF(h, \nu, \theta) = \frac{\gamma[T(h), p(h), \nu]}{\cos \theta}\, e^{-\tau(h, \nu, \theta)} \tag{3}$$

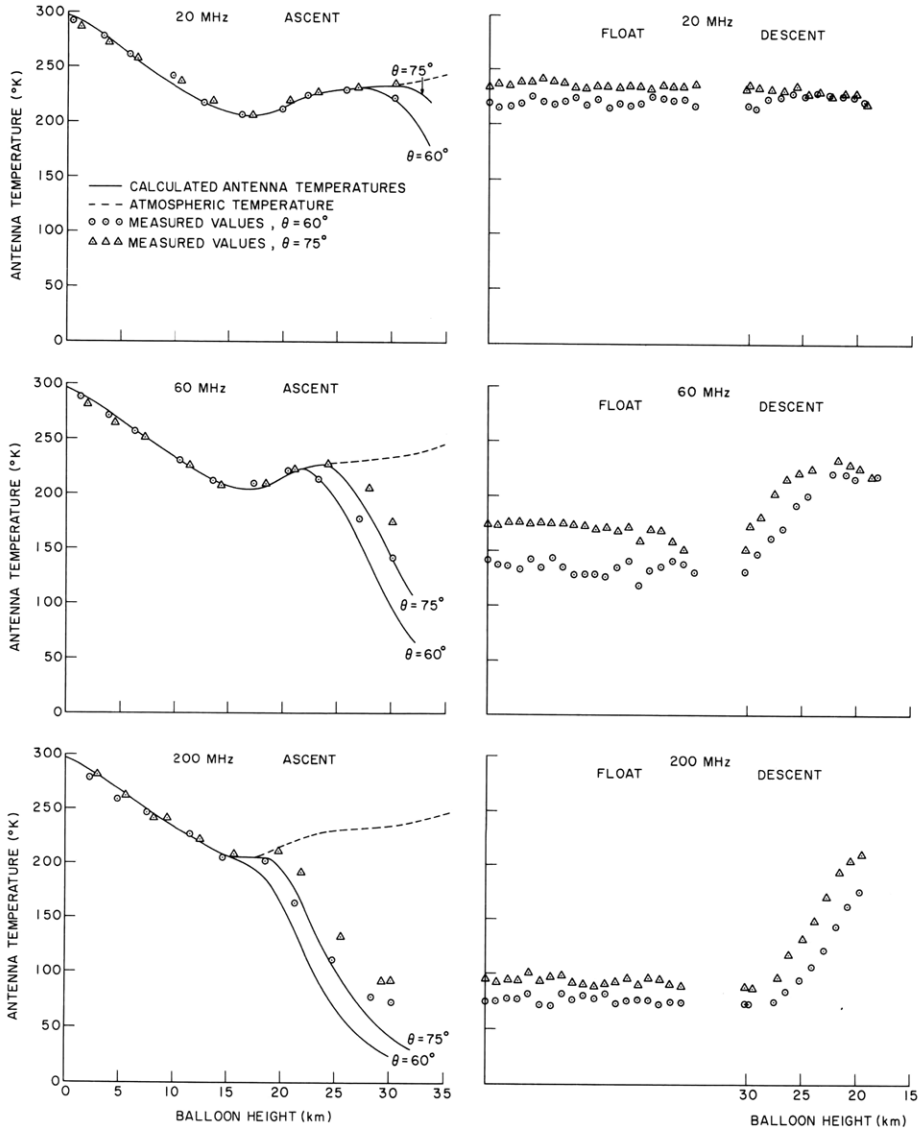

Fig. VI-6. Comparison of experimentally determined antenna temperature with computed values.

Table VI-4. Summary of Flights 152-P and 153-P.

ν_o = 61.151 GHz (9^+ resonance line)

ν_{if} = center frequency of IF passband

B_{if} = bandwidth of IF passband

θ = nadir angle of antenna axis

ΔT_{rms} = output noise fluctuations (measured)

θ (deg)	ν_{if} (MHz)	B_{if} (MHz)	ΔT_{rms} (°K)
60	20	10	1.6
60	60	10	2.8
60	200	15	1.4
0	20	10	2.4
0	60	10	3.5
0	200	15	2.3

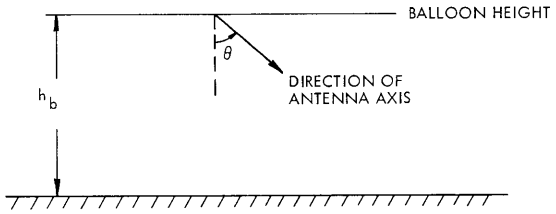

Fig. VI-7. Geometry of Flights 152-P and 153-P.

$$\tau(h, \nu, \theta) = \frac{\int_{A_b}^{h} \gamma[T(\xi), p(\xi), \nu]\, d\xi}{\cos \theta} \tag{4}$$

T(h) = atmospheric temperature at hight h

p(h) = atmospheric pressure at height h

γ = atmospheric attenuation coefficient.

Preliminary theoretical calculations are based on the use of the Van Vleck-Weisskopf line shape in the expression for the attenuation coefficient. Other parameters are the same as those used by Meeks and Lilley[5] and Barrett, et al.[6]

No useful data for the ascent part of Flight 150-P were taken, because of an equipment problem. Float and descent data are difficult to reduce for this flight, since final calibration temperatures are determined during the ascent part of the flight

Flight 154-P was successful in every respect. The experimentally determined antenna temperatures are compared with the computed values in Fig. VI-6. In the report in Section VI-D the inference of the atmospheric absorption coefficient from these measured antenna temperatures is discussed.

2. Results of Flights 152-P and 153-P

This pair of flights had the characteristics and geometry depicted in Fig. VI-7 and Table VI-4. Equation 1 ist still valid for T_A but T_B is given by

$$T_B(\nu, \theta) = \int_0^{h_0} T(h)\, WF(h, \nu, \theta)\, dh \tag{5}$$

with

$$WF(h, \nu, \theta) = \frac{\gamma[T(h), p(h), \nu]}{\cos \theta} e^{-\tau(h, \nu, \theta)} \tag{3}$$

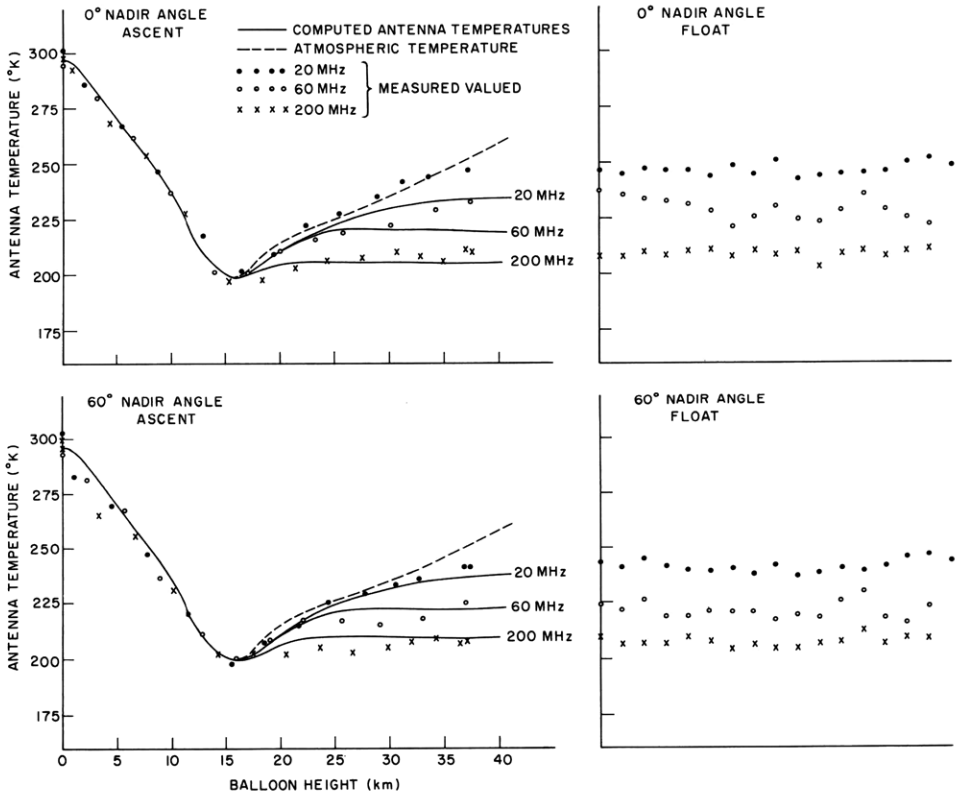

Fig. VI-8. Measured antenna temperatures for ascent and float parts of Flight 152-P.

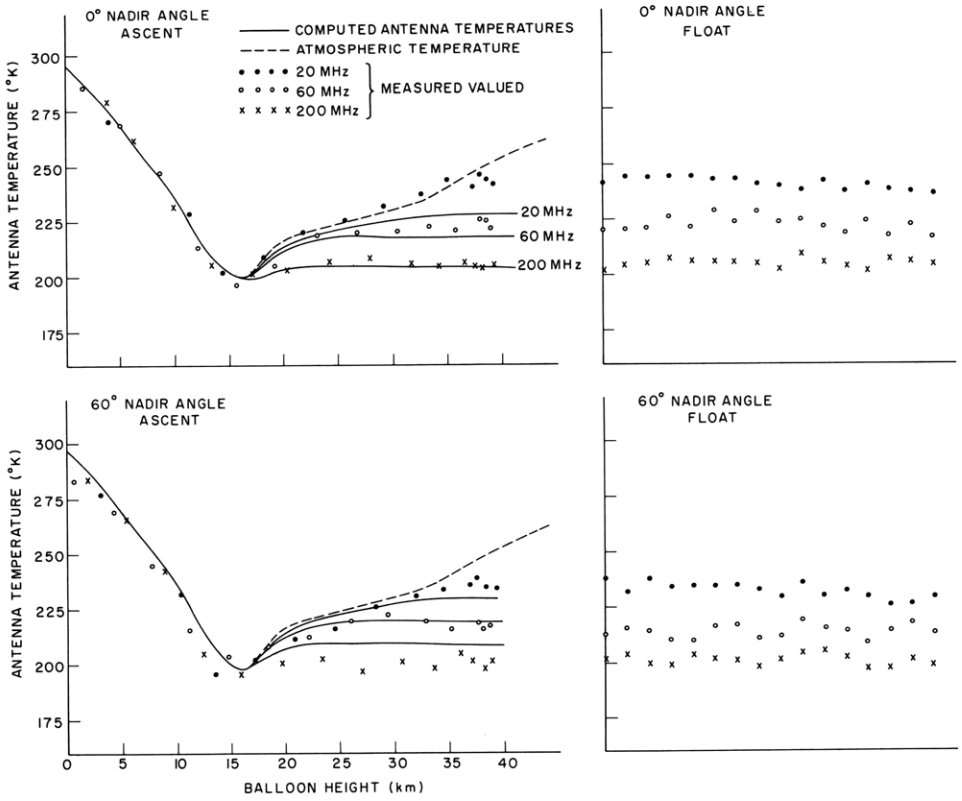

Fig. VI-9. Measured antenna temperatures for ascent and float parts of Flight 153-P.

$$\tau(h, \nu, \theta) = \frac{\int_h^{h_b} \gamma[T(\xi),\ p(\xi), \nu]\, d\xi}{\cos\theta}, \tag{6}$$

and all other parameters are the same as before.

The measured antenna temperatures for the ascent and float part of Flights 152-P and 153-P are presented in Figs. VI-8 and VI-9. Inferences of the atmospheric temperature profile based on these antenna temperature measurements will be made in the future, and the inferred profile will be compared with the profile resulting from measurements made during ascent.

W. B. Lenoir

References

1. W. B. Lenoir, Quarterly Progress Report No. 79, Research Laboratory of Electronics, M.I.T., October 15, 1965, pp. 17-19.
2. W. B. Lenoir, Quarterly Progress Report No. 82, Research Laboratory of Electronics, M.I.T., July 15, 1966, pp. 36-41.

3. J. H. Van Vleck, Phys. Rev. 71, 413 (1947).

4. J. H. Van Vleck and V. F. Weisskopf, Rev. Mod. Phys. 17, 227 (1945).

5. M. L. Meeks and A. E. Lilley, J. Geophys. Res. 68, 1683-1703 (1963).

6. A. H. Barrett, J. W. Kuiper, and W. B. Lenoir, J. Geophys. Res. 71, 4723-4734 (October 15, 1966).